

**Introduction to Direct Modulation of a Symmetrical Half-
Wavelength Patch Antenna Using Integrated Schottky Diodes**

Steven D. Keller

January 23, 2006

10:00AM – 11:30AM

**Prepared for the Duke University Department of Electrical and Computer
Engineering Ph.D. Qualifying Exam**

Dr. William T. Joines Dr. Qing Liu Dr. Hisham Massoud Dr. David Smith

Table of Contents

I.	Introduction	1
II.	Background Theory	
	A. Microstrip Patch Antenna	2
	B. Direct Antenna Modulation	
	1. General Concept	7
	2. Research History	9
III.	Patch Antenna Design	
	A. Theoretical Calculations	12
	B. HFSS Model Simulation	17
	C. Construction and Testing	22
IV.	Conclusion and Future Research	24
V.	References	27
VI.	Appendices	
	A. MATLAB Code	28

I. Introduction

Since the conception of the first wireless communication system by Guglielmo Marconi in 1895, one of the major goals of antenna research has been to discover ways to maximize the information bandwidth available to the antenna and at the same time maintain high radiation efficiency and keep its physical size to a minimum at any desired resonant frequency. However, tradeoffs between these desired characteristics are often necessary during antenna design since antenna size/geometry generally controls the resonant frequency and since an antenna operating linearly at resonance with high radiation efficiency is intrinsically narrowband. The key to avoiding such tradeoffs lies in decoupling these antenna characteristics from one another. This separation can be accomplished by employing direct antenna modulation, a novel modulation technique that has only begun to be explored.

Direct antenna modulation involves driving an antenna at resonance with a high-frequency carrier wave signal and then modulating it directly with a transistor switch that is controlled by a low-frequency baseband information signal, encoded into a digital pulse train. By biasing the transistor, the pulse train controls the power output of the antenna and can effectively modulate the transmitted carrier wave in a number of ways, such as on-off keying and pulse-width or pulse-code modulation. Since the antenna operates at resonance, it maximizes its radiation efficiency, and at the same time, the information bandwidth is no longer directly dependent upon the resonant bandwidth of the antenna. Also, the antenna geometry is only responsible for the resonant frequency of the carrier wave and is decoupled from the information signal frequency. Consequently, low-frequency information signal transmissions can be accomplished with significantly smaller antennas.

The benefits offered by direct antenna modulation have been identified by Devereux Palmer of the Electronics Division of the US Army Research Office (ARO) and a proposal has been submitted and accepted to explore this antenna modulation technique further. According to this proposal [6], "Because 80% of Army ground communications occurs below 1 GHz with dipole antennas that can be several meters in length, the result-

ing reduction in visual signature [due to the implementation of direct antenna modulation] could be immense.” With the incentive of smaller, less impeding antennas and an increase in information bandwidth beyond that of a linearly-operating resonant antenna, the ARO has agreed to fund research on this topic until August 2008.

This paper will describe the basic theory of direct antenna modulation and will give a thorough description of the research done to date on implementing and developing it. A review of patch antenna theory and a discussion on the design and testing of a symmetrical patch antenna for use in an upcoming direct antenna modulation experiment will also be presented. This experiment will be conducted in the 1st quarter of 2006, for publication as a Masters thesis in April 2006, and will involve the modulation of a square patch antenna with Schottky diodes and a comparison of such a modulation technique with that of a basic amplitude modulation technique.

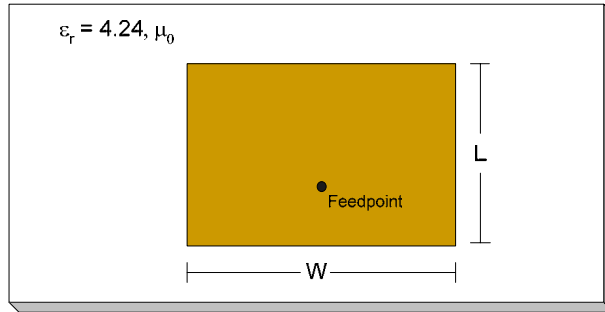
II. Background Theory

A. Microstrip Patch Antenna

The radiating element that was designed for this study to demonstrate the direct antenna modulation concept was a square half-wavelength microstrip patch antenna with a resonant frequency of 1.5 GHz. Since the square patch antenna is a special case of the rectangular patch antenna, the general theory for the rectangular microstrip patch antenna will be discussed in this section.

An example of a rectangular microstrip patch antenna is shown in Fig. 1. This antenna can be driven by a number of different signal-feeding methods, including a microstrip line, a coaxial probe, and a variety of coupling techniques including aperture and proximity-coupling. The design for this paper employed the coaxial probe feed, which is known for its ease of fabrication and input impedance matching, and for its low spurious radiation. [1]

Top view



$$L \approx \frac{\lambda_0}{2}$$

W = variable

$$h = \frac{1}{16}''$$

Side view

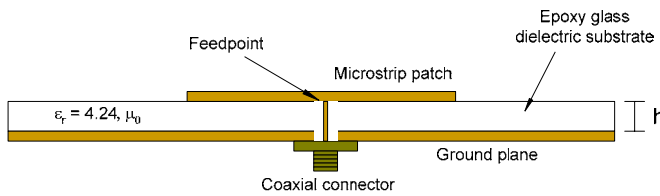


Fig. 1. Rectangular microstrip patch antenna with coaxial feed.

The rectangular patch antenna can be represented by a transmission line model of two narrow radiating apertures separated by a transmission line with a length and width equal to that of the patch antenna and with characteristic impedance Z_{01} (and corresponding characteristic admittance Y_{01}), as shown in Fig. 2.

The radiating apertures on the edges of the patch antenna are each represented by an admittance Y_{L1} and Y_{L2} , where $Y_{L1} = G_1 + jB_1$ and $Y_{L2} = G_2 + jB_2$. Since the radiating apertures are identical, the aperture conductances and susceptances are equal ($G_1 = G_2$, $B_1 = B_2$), and consequentially, the aperture admittances are equal ($Y_{L1} = Y_{L2} = Y_L$). The input signal feedpoint is located at a point along the length of the transmission line that is chosen to minimize the antenna reactance and maximize the input impedance match (50Ω for a typical coaxial feed).

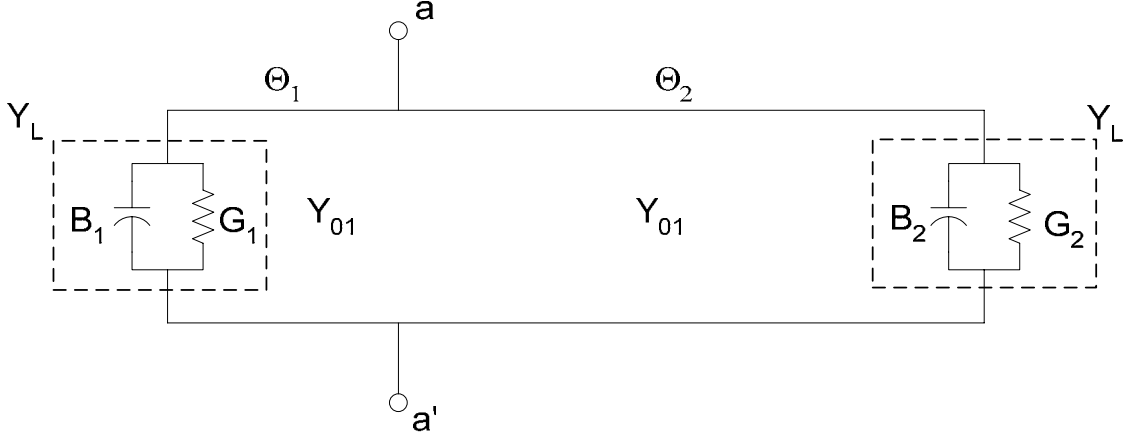


Fig. 2. Transmission line model of rectangular patch antenna.

According to transmission line theory,

$$Y_{aa'} = Y_{01} \cdot \frac{Y_L + jY_{01} \tan(\theta_1)}{Y_{01} + jY_L \tan(\theta_1)} + Y_{01} \cdot \frac{Y_L + jY_{01} \tan(\theta_2)}{Y_{01} + jY_L \tan(\theta_2)},$$

$$\theta_1 = \beta \cdot \ell_1, \quad \theta_2 = \beta \cdot \ell_2$$

$$\beta = \frac{2\pi}{\lambda_0}$$

where $Y_{aa'}$ represents the input admittance at the signal feedpoint. The length of the patch antenna, corresponding to a transmission line of electrical length $\theta_1 + \theta_2$, is set to approximately $\frac{\lambda_0}{2}$ so that the electric field polarization at each radiating aperture is opposite to the other. This maximizes broadside radiation above the patch and results in a negligible susceptance B_1, B_2 in the load admittance, Y_L , such that $Y_L \approx G_L$. The electric field polarization reversal effect is illustrated in Fig. 6, located in Section III.A.

If θ_1 is set to 45° , or $\frac{\lambda_0}{8}$, and θ_2 is set to 135° , or $\frac{3\lambda_0}{8}$, then the reactive component of $Y_{aa'}$ disappears and the formula for $Y_{aa'}$ reduces to,

$$Y_{aa'} = \frac{4 \cdot Y_{01}^2 \cdot G_L}{Y_{01}^2 + G_L^2}$$

The reciprocal of $Y_{aa'}$ yields a feedpoint impedance of,

$$Z_{aa'} = \frac{1}{4} \cdot \left(\frac{1}{G_L} + Z_{01} \cdot G_L \right)$$

Since the feedpoint impedance should equal 50Ω and both G_L and Z_{01} include the transmission line width, W , as a variable, the width that yields the best impedance match can be solved for by setting $Z_{aa'} = 50\Omega$ and solving for W in the following way:

From basic transmission line theory,

$$Z_{01} = \sqrt{\frac{L}{C}}$$

and from Schwarz-Christoffel transformations applied to a standard microstrip transmission line geometry,

$$C = \varepsilon \cdot F(g), \quad L = \frac{\mu}{F(g)}$$

$$F(g) = \frac{2 \cdot W}{h} + \frac{2}{\pi} + \frac{2}{\pi} \cdot \ln \left(1 + \frac{\pi \cdot W}{h} \right)$$

So Z_{01} simplified as a function of h and W results in,

$$Z_{01} = \frac{\sqrt{\frac{\mu}{\varepsilon}}}{\frac{2 \cdot W}{h} + \frac{2}{\pi} + \frac{2}{\pi} \cdot \ln \left(1 + \frac{\pi \cdot W}{h} \right)}$$

Next, from aperture antenna theory derived fully in [1], the aperture conductance G_L is approximated by means of a Fourier transform as,

$$G_L = \frac{W}{120 \cdot \lambda_0} \left[1 - \frac{1}{24} \cdot (\beta_0 \cdot h)^2 \right], \quad \beta_0 = \omega \sqrt{\mu \varepsilon}$$

By utilizing MATLAB, the above formula can be solved and optimized for the desired center frequency to yield a well-matched rectangular patch antenna, with an approximate length of $\frac{\lambda_0}{2}$, by setting Z_{aa} equal to 50Ω and solving for the antenna width, W . See ‘Variable_Width_Patch_Antenna.m’ in Section VI, Appendix A, for the code written to perform this task. Note that the following commonly-used formula for the effective dielectric constant, ϵ_{eff} , of the microstrip patch antenna [1] was substituted for the relative dielectric constant, ϵ_r , in the equation for Z_{01} ,

$$\epsilon_{eff} = \frac{\epsilon_r + 1}{2} + \frac{\epsilon_r - 1}{2} \cdot \left[1 + 12 \cdot \frac{h}{W} \right]^{-0.5}$$

This equation was determined empirically from experimentation and cannot formally be derived. The resulting plot in Fig. 3 shows that a width of $\sim 11.99\text{cm}$ will result in an optimal feedpoint impedance match of 50Ω for a 1.5 GHz rectangular patch antenna, with a length of $\frac{\lambda_0}{2}$ and feedpoint location of $\theta_1 = \frac{\lambda_0}{8}$.

Since the antenna designed for this study is a square patch antenna, the length and width are both approximately equal to $\frac{\lambda_0}{2}$ and the design procedure for such an antenna will consequent branch from the part of the transmission line theory discussed in this section. Instead of using a feedpoint located at exactly $\theta_1 = \frac{\lambda_0}{8}$, the feedpoint location must be experimentally tuned to a new length, θ_1 , where Z_{aa} approximately equals 50Ω for $W = L = \frac{\lambda_0}{2}$. Section III. A. will detail the design procedure for the square patch antenna.

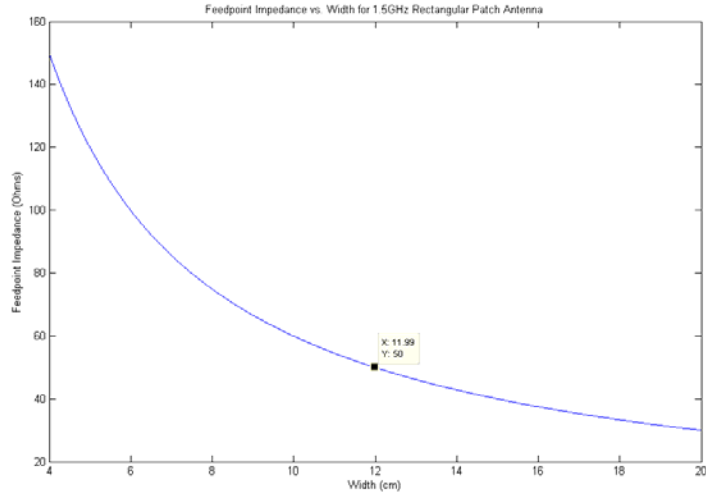


Fig. 3. Graphical solution for feedpoint impedance-matching by width variation.

B. Direct Antenna Modulation

1. General Concept

Direct antenna modulation involves the incorporation of high-speed semiconductor switching technology with a radiating element in order to decouple the information bandwidth and radiation efficiency from the limiting bandpass nature of a resonant antenna and to eliminate the reliance of antenna size and geometry on the desired information signal frequency. By applying transistor switching techniques similar to those described in a US patent on synthesizer radiating systems [4] and those utilized for high-efficiency Class-D amplifiers [3], a unique antenna modulation system can be employed. A basic implementation of direct antenna modulation is shown in Fig. 4.

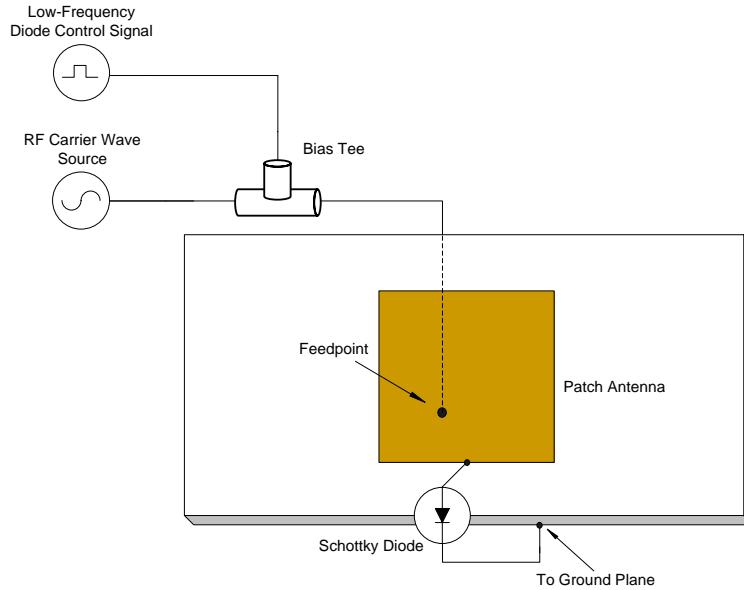


Fig. 4. Basic implementation of direct antenna modulation.

After an antenna is designed and constructed to operate at a desired resonant frequency, one or more high-speed semiconductor switches, such as Schottky diodes, are connected between the antenna and the ground plane. An RF carrier wave at the approximate resonant frequency of the patch antenna passes through a bias tee circuit and drives the antenna at resonance through a feedpoint. Simultaneously, a lower-frequency baseband information signal, in digital pulse train format, passes through the bias tee circuit to the feedpoint and controls the semiconductor switch. When the baseband signal has a value below that of the semiconductor junction voltage, V_d , the switch displays high resistance to the carrier wave-generated oscillating charges on the patch antenna and the antenna fully radiates the carrier wave. When the baseband signal has a value close to or higher than that of V_d , the switch opens and provides a direct path for the oscillating charges on the patch antenna to flow to ground, causing antenna radiation to effectively cease. [7] This allows the digital information signal to be directly modulated onto the carrier wave. The antenna always radiates at its resonant frequency, producing high radiation efficiency. Also, the antenna geometry and size are no longer dependent upon the baseband information signal frequency, but are mainly dependent upon the desired carrier wave frequency. As will be fully described below in the historical review of direct antenna

modulation research, the information bandwidth of the system is also decoupled from the resonant bandwidth of the antenna and is mainly limited by the switching characteristics of the incorporated diode. This results in a significant increase in the available information bandwidth, beyond that which is provided by a linearly-operating resonant antenna.

2. Research History

The scope of the literature review presented in this study has been limited to those papers which specifically employ the direct antenna modulation technique described above. However, it is also necessary to briefly address research conducted on the self-mixing antenna, since it resembles the direct antenna modulation technique and could be considered its predecessor. An example of such an antenna is described in [5], where a self-mixing inverted circular patch antenna was designed to operate at 6.25 GHz with a bandwidth of approximately 200 MHz. A Gunn diode oscillator was connected to the antenna in order to provide a simple self-mixing device. The low-frequency information signal was modulated onto the carrier wave within the Gunn diode, and this modulated carrier wave was then passed on to the antenna, where it was radiated at the resonant frequency. As a receiver, the Gunn diode provided the local oscillator (LO) element to demodulate the received carrier wave. An existing limitation, however, was that “because the RF signal transmitted is also used as the LO reference, simultaneous transmission and reception cannot take place.” [5] A self-mixing antenna of this design provides a convenient, compact self-mixing transceiver, but still limits the system bandwidth to the resonant bandpass nature of the antenna.

The first clear implementation of direct antenna modulation was conducted by Fusco and Chen in 1999 [2]. In this paper, a 10.09 GHz patch antenna was fabricated onto a high-resistivity silicon (HRS) substrate. The contact made between the patch antenna, HRS substrate, and metal ground plane was “equivalent to many metal-semiconductor barriers in shunt connection.” [2] This resulted in a distributed Schottky diode in shunt connection between the patch antenna and the ground plane, forming a fully-integrated direct antenna modulation system. By driving the patch antenna with a carrier wave at the resonant frequency of 10.09 GHz and then applying a DC bias voltage between the an-

tenna and the ground plane to control the integrated Schottky diode switch, a number of interesting discoveries were found that supported the concept of direct antenna modulation. Fusco and Chen found that as they increased the DC bias voltage from 0 to 5V, the radiated power of the patch antenna decreased by over 20 dB, while the radiation patterns of the E and H fields remained relatively unaffected. They also found that the resonant frequency of the patch antenna decreased and the resonance of the antenna became less effective as the DC bias voltage increased. From the captured S_{11} input reflection coefficient plots at 0V, 3.3V, and 4.8V, it could clearly be seen that the increased bias voltage caused a large increase in input signal reflections and caused the antenna radiation performance to steadily drop. These results implied that “by changing the bias voltage applied to the patch antenna, direct base-band data encoding by way of amplitude modulation of the RF carrier [could] be achieved.” [2] A simple square wave bias signal was applied to the radiating patch antenna in an attempt to modulate the resonant carrier wave. The results confirmed that direct antenna modulation was indeed possible, as the demodulated received signal showed that square wave had clearly been transmitted. As the frequency of the bias signal was increased, distortion and attenuation was observed in the received square wave. This ultimately limited the information frequency of the antenna to 20 kHz. Fusco and Qiang concluded that the main cause of this distortion and attenuation was the long fall-time of the Schottky diode switch, which was strongly influenced by the long carrier lifetime of the HRS substrate. Thus, an improved fall-time for the selected Schottky diode should yield a higher cutoff frequency for the information signal, and consequently, an increased information bandwidth.

With the feasibility of direct antenna modulation demonstrated by Fusco and Qiang [2], a modified implementation of this technique was recently conducted by Yao and Wang of UCLA [7]. A 2.4125 GHz rectangular patch antenna was constructed on a standard dielectric substrate and three discrete Schottky diode switches were soldered to its radiation slots to create a direct switching path between the antenna and the ground plane. By using a standard dielectric substrate and discrete Schottky diodes instead of an HRS substrate as in [2], the significant losses at microwave frequencies that occur within most silicon substrates was avoided. Using a -10 dB return loss standard, the patch antenna

had a reported bandwidth of 30 MHz. When a 100 Mbps square wave was externally modulated onto a 2.4125 GHz carrier wave and transmitted by the antenna, the received signal waveform exhibited a great deal of distortion since the signal bandwidth had greatly exceeded the antenna bandwidth and was causing dispersion. [7] However, when direct antenna modulation was employed and a 100 Mbps signal was used to control the antenna radiation by means of the Schottky diode switches, the received signal waveform exhibited little distortion and the transmitted square wave could clearly be demodulated from it. The effect of the diode switching characteristics on the clarity of the received waveform that was suggested in [2] was confirmed by this experiment. The received waveform exhibited a relatively longer rise-time than fall-time. This was in agreement with the observation that the reported fall-time of the Schottky diode used for this experiment, which was responsible for the closure of the diode switch and consequent enabling of antenna radiation, was longer than its rise-time. Thus, one conclusion drawn from this experiment was that the use of Schottky diodes with faster rise and fall-time characteristics could yield a noticeable improvement to the direct antenna modulation technique. Another observation that Yao and Wang noted from this experiment was that a small amount of the carrier wave signal was still transmitted by the patch antenna when the diode switch was open (information signal had a value above that of V_d) and the radiation from the transmitter patch antenna should have completely ceased. This small imperfection was attributed the finite 'ON'-state resistance of the Schottky diode switch, which did not allow all of the oscillating charges on the patch antenna radiation slots to dissipate to the ground plane. [7] From this paper, which is the most recent documented experiment conducted on direct antenna modulation, an increase in information bandwidth from approximately 30 MHz to over 200 MHz was reported --- an increase to over 6.5 times that of the reported antenna bandwidth.

Thus, the groundwork has been laid for further investigation of the direct antenna modulation technique. The apparent improvements that this modulation technique offers to antenna geometry and functionality strongly suggest that it should be investigated in more depth. As such, the following sections will thoroughly document the first step in an ARO research project on direct antenna modulation, which will involve verifying the general concept by conducting an experiment similar to that which is described in [7] and

then expanding upon it. The design and testing of a patch antenna for use in this upcoming experiment will be described in the following section.

III. Patch Antenna Design

A. Theoretical Calculations

In order to demonstrate direct antenna modulation, a well-designed antenna is necessary to serve as the transmitter and receiver in the basic communication system. As described in Section II A., a microstrip patch antenna is an efficient broadside radiating element that is reasonably easy to construct. Despite its relatively narrow bandwidth compared to other antenna geometries, the microstrip patch antenna is a reasonable antenna design for the first attempt at demonstrating direct antenna modulation.

While Section II A. discussed the general theory for a rectangular microstrip patch antenna, the design chosen for this experiment is a special case of this rectangular geometry, where $L = W = \frac{\lambda_0}{2}$. The resulting geometry is a symmetric microstrip patch antenna that utilizes both pairs of radiating apertures at the four edges of the patch. When a signal is fed into a certain point along the diagonal of such a patch antenna, where the feedpoint impedance Z_{aa} is approximately 50Ω and its reactance is minimized, broadside radiation is produced that is linearly-polarized in both the x and y-planes (with the z-plane orthogonal to the patch antenna), as opposed to being polarized in only the x or the y-plane, as is the case with a asymmetric rectangular patch antenna. Fig. 5 shows this effect.

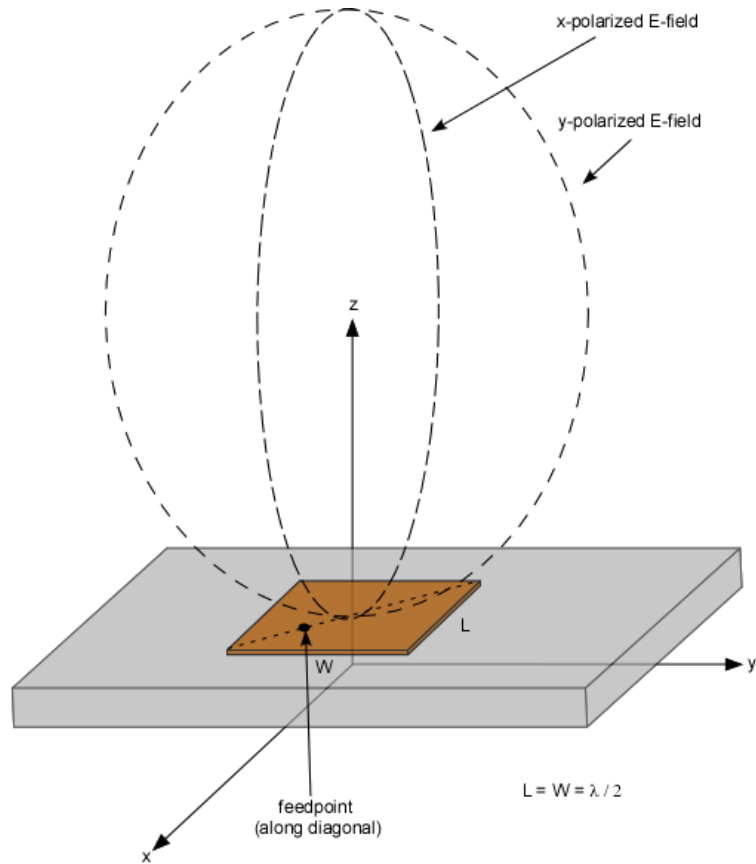


Fig. 5. Linearly-polarized E-fields for square patch antenna.

A center frequency of approximately 1.5 GHz was chosen for this experiment and G-10 epoxy glass dielectric boards were used as the antenna substrate. At 1.5 GHz, the dielectric constant, ϵ_r , for the substrate is approximately 4.24.

As a first step in the design of this square microstrip patch antenna, an optimal length L and width W were calculated that should result in a center frequency of approximately 1.5 GHz. As discussed in Section II A., this should be exactly $\frac{\lambda_0}{2}$,

$$L_0 = W_0 = \frac{1}{2 \cdot f_c \cdot \sqrt{\mu\epsilon_r}} = \frac{1}{2 \cdot 1.5 \cdot 10^9 \cdot \sqrt{4\pi \cdot 10^{-7} \cdot 4.24 \cdot 8.854 \cdot 10^{-12}}} \approx 4.85 \text{ cm}$$

However, the fringing electric fields on the edges of the patch antenna must be taken into account since they effectively increase the electrical length of the antenna, as shown in Fig. 6.

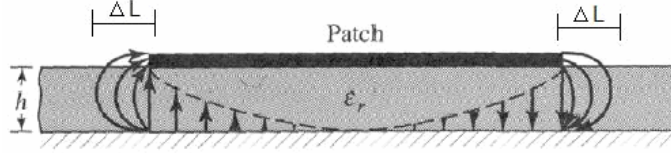


Fig. 6. Side view of patch antenna with fringing field effect.
(Adapted from [1], P. 729)

Thus, it is necessary to slightly decrease the physical length of the patch antenna such that $L = W < \frac{\lambda_0}{2}$ in order for the antenna to function at the desired center frequency. Similar to the formula for the effective dielectric constant presented in Section II A., a commonly-used equation for the fringing field contribution to the patch antenna length [1] was determined empirically by experimentation and cannot be formally derived,

$$\Delta L = 0.412 \cdot h \cdot \frac{(\epsilon_{eff} + 0.3) \cdot \left(\frac{W}{h} + 0.264\right)}{(\epsilon_{eff} - 0.258) \cdot \left(\frac{W}{h} + 0.8\right)}$$

where,

$$\epsilon_{eff} = \frac{4.24 + 1}{2} + \frac{4.24 - 1}{2} \cdot \left[1 + 12 \cdot \frac{h}{W}\right]^{-0.5}$$

After determining the fringing field contribution to the length, ΔL , the calculated physical length can be adjusted properly such that $L = W = L_0 - 2 \cdot \Delta L$. Since both the effective dielectric constant, ϵ_{eff} , and the fringing field contribution to the length, ΔL , both depend

on W , MATLAB was employed to find the value where $L = W \sim \frac{\lambda_0}{2}$ for a 1.5 GHz patch antenna with the fringing field taken into account. See ‘Square_Patch_Dimensions.m’ in Section VI, Appendix A, for the code written to perform this task. The resulting plot in Fig. 7 shows that an approximate value of $L = W = 4.71$ cm will yield an optimal square patch antenna operational at 1.5 GHz.

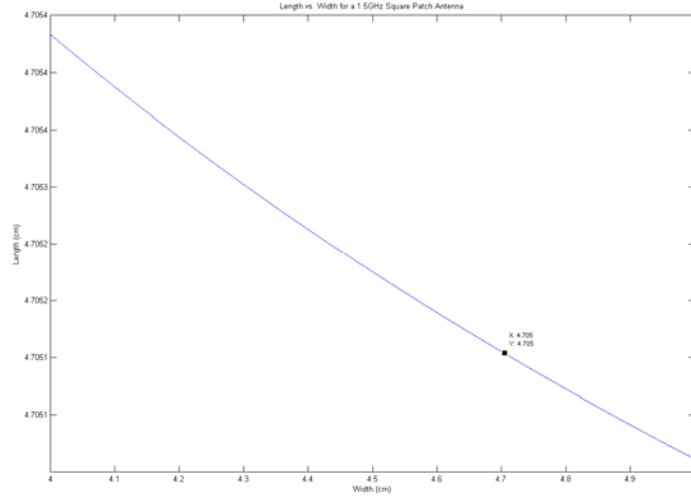


Fig. 7. Graphical solution for the physical dimensions of a 1.5 GHz square patch antenna.

With the physical dimensions of the patch antenna determined, a location along the diagonal of the antenna must be chosen where the feedpoint impedance $Z_{aa'} = 50\Omega$ and its reactance is minimized. By calculating the feedpoint admittance described in Section II A., the feedpoint impedance can be found as $Z_{aa'} = \frac{1}{Y_{aa'}}$. The equations for Z_{01} , G_L , and $Z_{aa'}$ (from Section II A.) were solved in MATLAB for the optimized width $W = 4.71$ cm and for $0 \leq \theta_1 \leq \frac{\pi}{2}$. See ‘Square_Patch_Feedpoint.m’ in Section VI, Appendix A, for the code written to perform this task. The resulting plot in Fig. 8 shows that an approximate value of $\theta_1 = 63.7^\circ$ will yield a feedpoint impedance $Z_{aa'} \sim 50\Omega$.

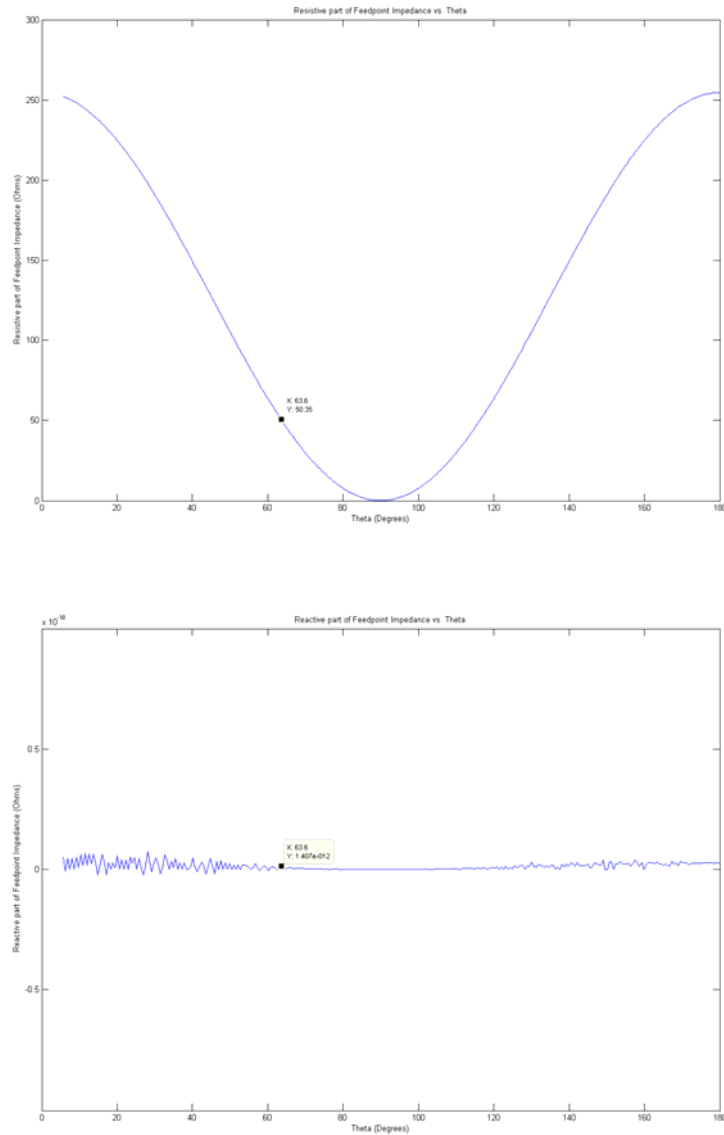


Fig. 8. Graphical solution for feedpoint impedance of square patch antenna.

Note that this technique approximates the patch antenna physical length by $\frac{\lambda_0}{2}$, which is relatively imprecise due to the fringing field effect. However, the results from this technique do give an acceptable approximation of the optimal feedpoint location.

The location of this feedpoint along the physical length of the patch is determined as,

$$\ell = \frac{\theta_1}{180^\circ} \cdot W = \frac{63.7^\circ}{180^\circ} \cdot 4.71 = 1.67 \text{ cm}$$

From this feedpoint location along the length, the diagonal feedpoint along the square patch antenna can be calculated as,

$$\ell_{\text{diagonal}} = \sqrt{\ell^2 + \ell^2} = \sqrt{2 \cdot 1.67^2} = 2.36 \text{ cm}$$

Thus, the initial design of the 1.5 GHz square microstrip patch antenna has been calculated, with the length, width, and feedpoint along the diagonal determined from antenna theory. Fig. 9 shows the design, before experimental fine-tuning.

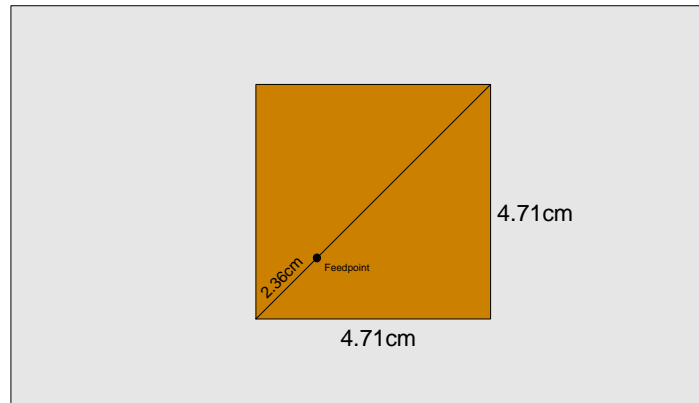


Fig. 9. Square patch antenna design (theoretical result).

B. HFSS Model Simulation

Following the successful calculation of the theoretical design, the patch antenna dimensions and feedpoint were fine-tuned through model simulations using *Ansoft* High Frequency Structure Simulator (HFSS). A model of the symmetrical microstrip patch antenna was constructed in HFSS, as shown in Fig. 10. The copper ground plane on the bottom surface of the substrate was approximated as an infinite perfect electric conducting (PEC) ground plane, while the patch antenna above the substrate was approximated as an actual copper tape slab, with a thickness of 88 μm . The substrate was modeled after

a 7.6 x 15.2 cm G-10 epoxy glass board with a thickness of 1/16" and dielectric constant at 1.5 GHz of 4.24.

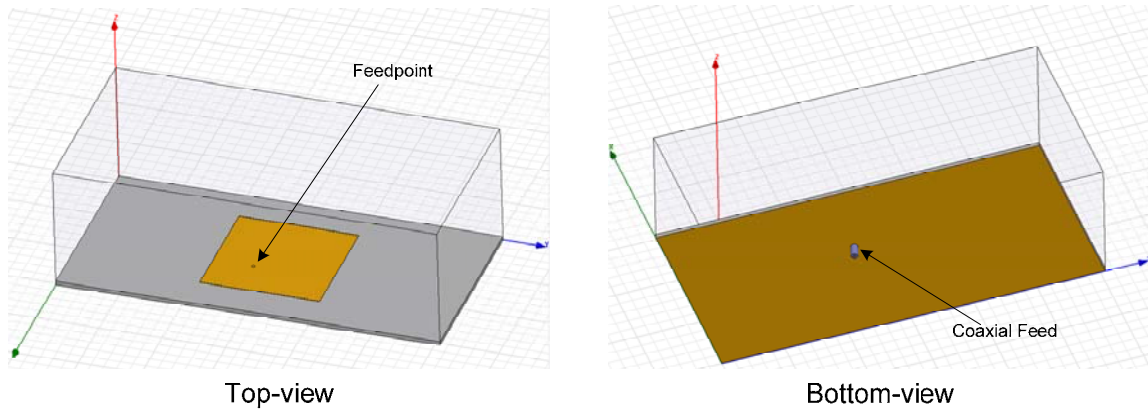


Fig. 10. HFSS model of symmetric microstrip patch antenna.

The dimensions of the symmetric patch antenna model were experimentally tuned between 4.71 cm and 4.78 cm and a fast sweep simulation was run from 1 GHz to 2 GHz, with field solutions centered on 1.5 GHz to examine the electric field variation along the patch at the desired center frequency. The S11 response of the antenna model, detailing the amount of power reflected from the coaxial line feedpoint, was analyzed for these different antenna dimensions to see which dimension value yielded a resonant frequency closest to 1.5 GHz. The feedpoint was also adjusted to maximize the feedpoint impedance match. The S11 response for $L = W = 4.71$ cm, which was the theoretical result calculated in Section III A., showed that the simulated resonant frequency was slightly higher than 1.5 GHz, being ~ 1.515 GHz. A patch antenna model with $L = W = 4.76$ cm and a feedpoint at ~ 2.38 cm along the patch diagonal yielded a resonant frequency much closer to 1.5 GHz, as well as an excellent resonant return loss. The S11 response for this model is shown in Fig. 11.

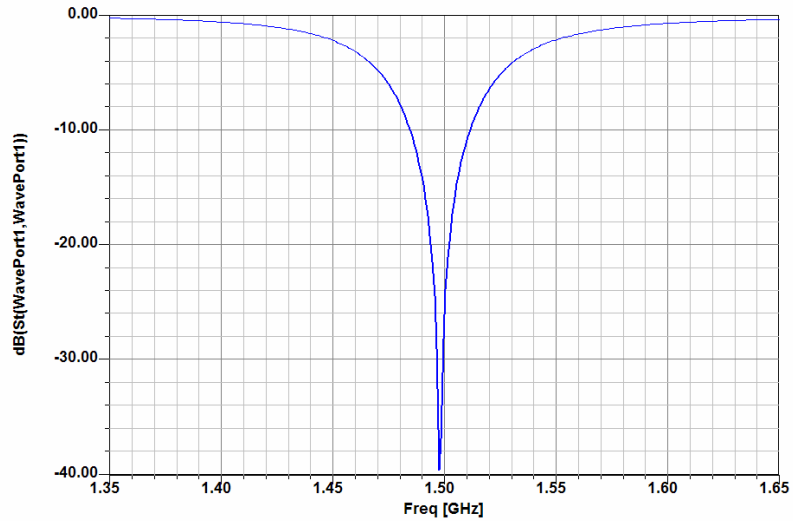


Fig. 11. S11 response for HFSS simulation of microstrip patch antenna ($L = W = 4.76\text{cm}$).

According to the simulation, a very good impedance match occurs between the antenna feedpoint and the coaxial feed at $\sim 1.496\text{ GHz}$, with a return loss of -39.5 dB . This can also be seen by examining a plot of the feedpoint resistance and reactance vs. frequency, as shown in Fig. 13 and Fig. 13. At $\sim 1.496\text{ GHz}$, the feedpoint resistance approximately equals the characteristic impedance of the coaxial feed ($\sim 49.96\Omega$) and the feedpoint reactance magnitude is minimized.

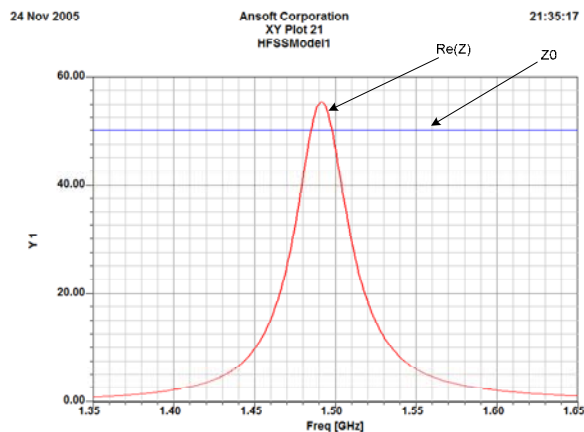


Fig. 12. Feedpoint resistance for HFSS simulation of microstrip patch antenna ($L = W = 4.76\text{cm}$).

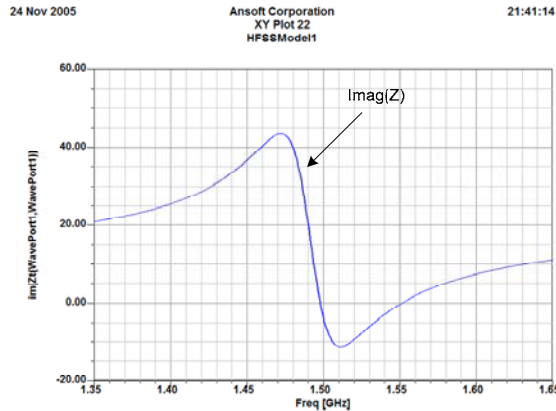


Fig. 13. Feedpoint reactance for HFSS simulation of microstrip patch antenna ($L = W = 4.76\text{cm}$).

When direct antenna modulation is implemented with this patch antenna design, the Schottky diodes should be placed at locations between the antenna and the ground plane where the electric field is at its highest value. This should maximize the switching effect of the integrated diodes and consequently yield the cleanest modulation effect. E-field magnitude and vector plots from the HFSS simulation results were used to find these points.

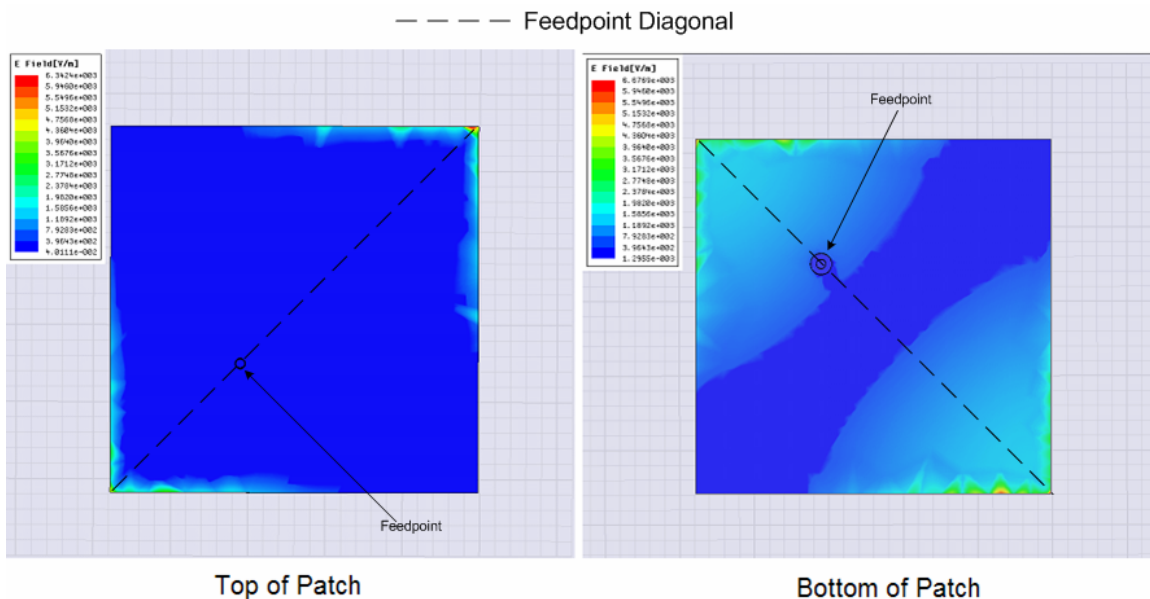


Fig. 14. E-Field magnitude overlay for HFSS simulation of microstrip patch antenna ($L = W = 4.76\text{cm}$).

The E-field magnitude plot for the patch antenna prototype is shown in Fig. 14. The highest points of the electric field appear to occur near two of the corners of the square patch, along the feedpoint diagonal. When the Schottky diodes are integrated with the patch antenna in an upcoming direct antenna modulation experiment, they will be placed at those locations.

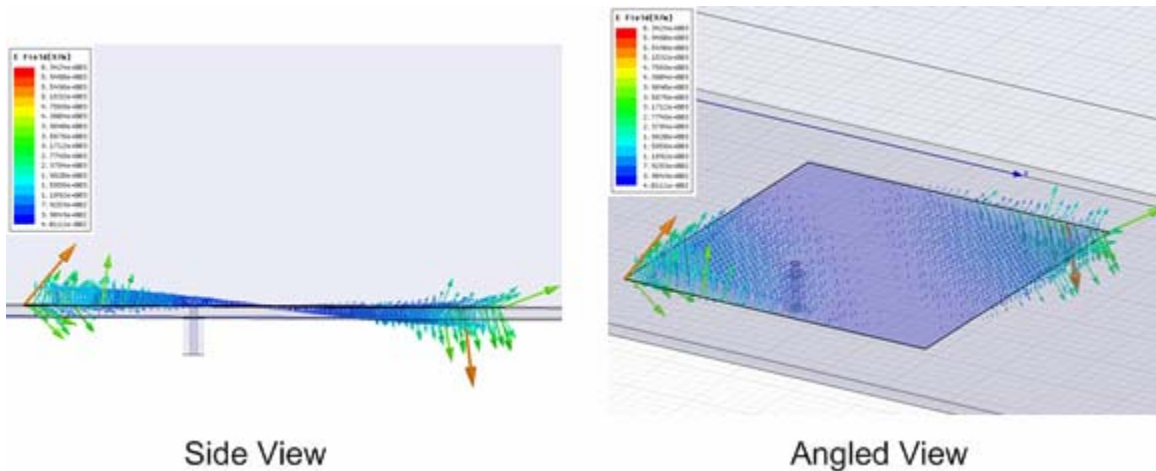


Fig. 15. E-Field vector overlay for HFSS simulation of microstrip patch antenna ($L = W = 4.76\text{cm}$).

The E-field vector plots shown in Fig. 15 confirm the locations of the highest electric field points. This plot also confirms the theory discussed in Section II.A. regarding how the electric field at each end along the feedpoint of a $\frac{\lambda}{2}$ patch antenna is 180° out of phase with the opposite end. It is this reversal in polarization that results in the broadside radiation pattern, which is shown in the HFSS-simulated far-field radiation plot in Fig. 16.

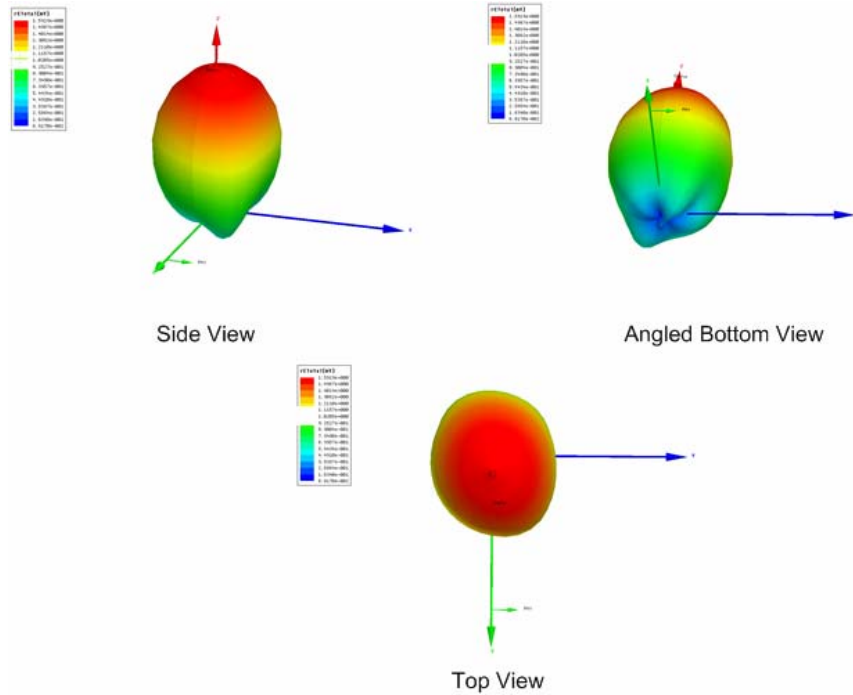


Fig. 16. Far-field radiation plot for HFSS simulation of microstrip patch antenna ($L = W = 4.76\text{cm}$).

The far-field radiation plot looks reasonable for the simulated patch antenna design. The broadside radiation pattern formed above the patch agrees well with the theory described in Section II.A., although it appears to be slightly elliptical from the top-view. The top-view radiation pattern appears to be slightly shorter in radius along the feedpoint diagonal than along the opposite diagonal. This is most likely due to the square shape of the patch antenna, which yields radiation linearly-polarized in both the x-plane and the y-plane, as opposed to a single linear polarization.

C. Construction and Testing

Having successfully simulated the design for a symmetrical 1.5 GHz patch antenna in HFSS, a prototype antenna was constructed and tested. A 10.1 x 15.2 cm single-sided copper clad G-10 epoxy glass board from *MG Chemicals* was used as the dielectric substrate for the prototype. A roll of 3" EMI copper foil with conductive adhesive tape from *3M* was used to construct the patch antenna on the G-10 epoxy glass substrate.

After a number of trial runs and adjustments to the patch antenna dimensions and feed-point location, a satisfactory result was achieved with a length and width of ~ 4.8 cm and the feedpoint placed ~ 1.84 cm along the diagonal. The antenna was simulated using a *Hewlett-Packard* 8753A Network Analyzer. The experimental setup is shown in Fig. 17. The resulting return loss plot can be seen in Fig. 18.

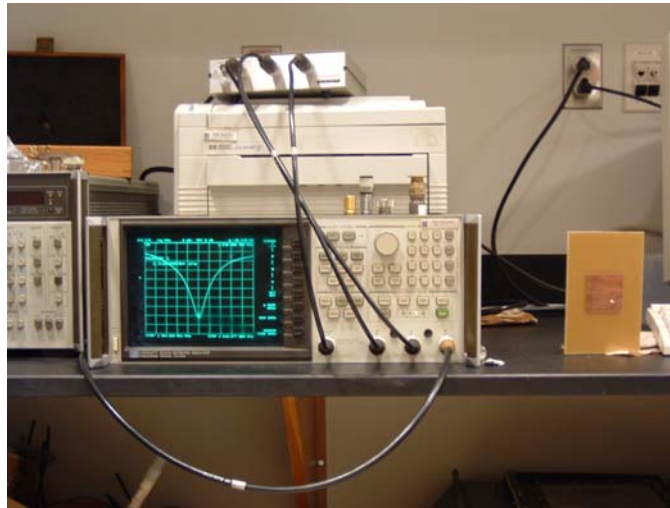


Fig. 17. Experimental setup of S11 return loss measurement with *HP* 8753A network analyzer

From this return loss plot, the resonant bandwidth of the antenna was determined as follows:

$$1536.23 \text{ MHz} - 1500.07 \text{ MHz} = 36.16 \text{ MHz} \quad (\text{using a } -10\text{dB return loss standard})$$

$$1524.18 \text{ MHz} - 1513.11 \text{ MHz} = 11.07 \text{ MHz} \quad (\text{using a } -15\text{dB return loss standard})$$

The variation of the relative dielectric constant of the substrate, ϵ_r , from its estimated value of 4.24 most likely had a strong effect on the discrepancy between the experimental resonant frequency and the theoretically predicted and simulated values. In addition to this, experimental approximations in the construction and testing of the antenna also were significantly responsible for such a discrepancy.

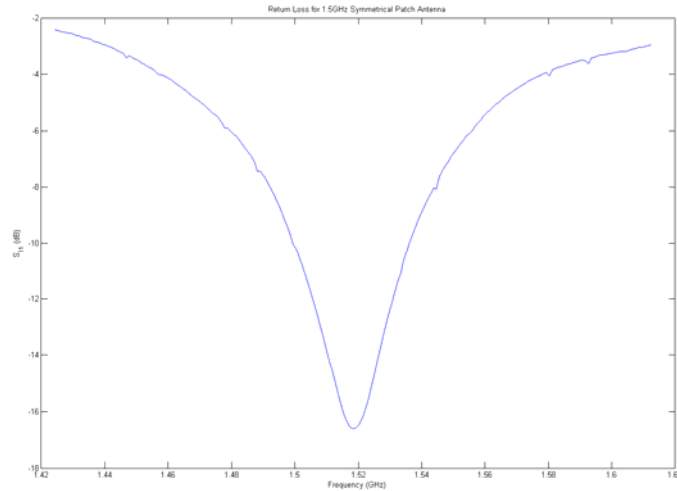


Fig. 18. S11 return loss plot for symmetrical patch antenna prototype

IV. Conclusion and Future Work

The 1.5 GHz patch antenna design that was determined by simulation and experimental fine-tuning for this project should work well as a radiating element in the upcoming experiment to implement direct antenna modulation. With a narrow resonant bandwidth of ~ 36 MHz, there is significant room for improvement that direct antenna modulation can offer to the information bandwidth of a communication system that utilizes such an antenna. By driving the antenna at resonance and directly modulating it with an integrated Schottky diode being biased by an external pulse train, the frequency of this external modulating signal should be able to far exceed the resonant bandwidth of the antenna and still produce a clear demodulated waveform at the receiving end of a basic communication system. Such a communication system has been tested using this antenna design, but the crystal detector being used to strip off the envelope of the modulated carrier wave signal is inadequate for the desired testing range of the information signal frequency. As shown in Fig. 19, a demodulated square wave signal becomes significantly distorted and reduced to $\frac{1}{2}$ of its peak-to-peak voltage at only ~ 185 kHz using the available *Alfred Electronics* crystal detector Model 1001. A new crystal detector has been ordered that will hopefully produce minimal distortion to the demodulated signal for modulating frequencies up to at least 100-200 MHz. Since the current results of this basic communica-

tion system test are severely limited by the available crystal detector, a detailed discussion of the test and results will be saved for a later time.

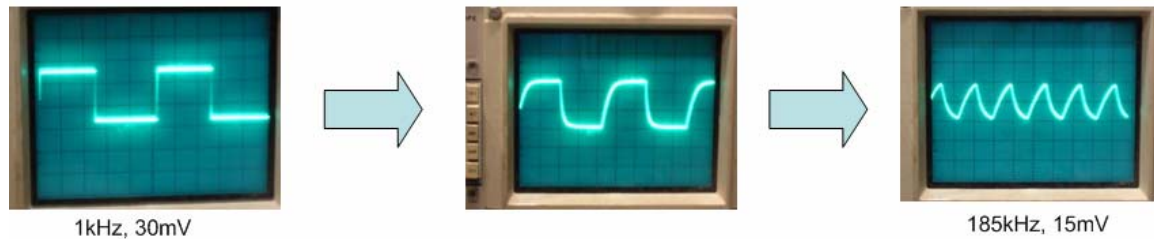


Fig. 19. Distortion of demodulated information signal using currently-available crystal detector

Once a suitable crystal detector is obtained, a simple direct antenna modulation system will be constructed and tested using available lab equipment. Based on the promising results of prior experiments pertaining to direct antenna modulation discussed in Section II. B. 2., a significant improvement in the available information bandwidth should be observed, when compared to that of a simple amplitude-modulated system.

After this first demonstration of direct antenna modulation is accomplished, a number of subsequent research topics on direct antenna modulation will be explored. Currently, direct antenna modulation is only proven to employ basic on/off keying, amplitude modulation, and pulse-width/pulse-code modulation. One question that must be addressed is whether direct antenna modulation can be used to employ n-level quadrature amplitude modulation (nQAM) and quadrature phase shift keying (QPSK) modulation schemes. According to technical staff at the ARO, these modulation schemes are widely used by Army mobile wireless communication systems, so it will be crucial to try to employ them using direct antenna modulation.

Another key part of the investigation of direct antenna modulation will be to develop methods to accurately model and predict direct antenna modulation performance. This will include the development of computational models using an EM simulation program such as HFSS and potentially the development of a nonlinear circuit model that could be

employed with a circuit-modeling program such as HSPICE, PSPICE etc. By accurately modeling and experimenting with the technique, I will hopefully be able to develop an analytical model that fully describes the direct antenna modulation concept.

Finally, after developing models of the direct antenna modulation technique applied to high-frequency antennas, the technique will then be applied to antennas operating in the HF/VHF/UHF carrier wave frequency ranges, since many Army ground communication systems operate in these frequency ranges (less than 1 GHz).

With the successful conclusion of this research on direct antenna modulation in 2-3 years, a novel modulation technique will be available to the Army that should significantly improve the operational bandwidth of their low-frequency ground communication systems. The groundwork for this research has been laid out in this paper with the development of a suitable radiating element, a symmetrical 1.5 GHz patch antenna, and the introduction to the direct antenna modulation technique, with an overview of its theory, a review of the research done on the topic to date, and the direction of future research that will be conducted to further explore this promising technique.

V. References

- [1] C. A. Balanis, Antenna Theory: Analysis and Design, 2nd Edition, pp. 722 – 752, John Wiley and Sons, Inc., 1997.
- [2] V. F. Fusco and Q. Chen, “Direct-signal Modulation Using a Silicon Microstrip Patch Antenna,” *IEEE Trans. Antennas and Propagation*, vol. 47, no. 6, pp. 1025 – 1028, June 1999.
- [3] T.-P. Hung, A. G. Metzger, P. J. Zampardi, M. Iwamoto, and P. M. Asbeck, “Design of High-Efficiency Current-Mode Class-D Amplifiers for Wireless Handsets,” *IEEE Trans. Microwave Theory and Techniques*, vol. 53, no. 1, pp. 144-151, January 2005.
- [4] J. T. Merenda, “Synthesizer Radiating Systems and Methods”, United States Patent Number 5,402,133, Mar. 28, 1995.
- [5] C. M. Montiel, L. Fan, and K. Chang, “A Novel Active Antenna with Self-Mixing and Wideband Varactor-Tuning Capabilities for Communication and Vehicle Identification Applications,” *IEEE Trans. Microwave Theory and Techniques*, vol. 44, no. 12, pp. 2421 – 2430, December 1996.
- [6] W. D. Palmer, “Direct Antenna Modulation: Analysis, Design, and Experiment”, Electronics Division, US Army Research Office, Research Proposal, pp. 1 – 11, July 2005.
- [7] W. Yao and Y. E. Wang, “An Integrated Antenna for Pulse Modulation and Radiation,” *Conf. Rec. 2004 IEEE Radio and Wireless Conference*, pp. 427-429.

VI. References

A. MATLAB Code

Variable Width Patch Antenna.m

```
clear all; close all;

%Define Constants
er = 4.8;      %Relative dielectric constant of substrate
mu0 = 4*pi*10^-7;
e0 = 8.854*10^-12;
f = 1.5*10^9; %Center frequency of antenna (Hz)
h = 0.00159   %Thickness of substrate(m)
lambda0 = 1/ (sqrt(mu0*er*e0)*f); %Wavelength (m)

%Vary Width from 4cm to 20cm
W = 0.04:0.00001:0.2;

%Relative Dielectric Constant (from Empirically-Determined Formula [1])
ereff = (er + 1)/2 + ((er - 1)/2).*(1 + 12.*(h./W)).^-0.5;

%Characteristic Impedance of Transmission Line
Fg = 2.*W./h + 2/pi + (2./pi).*log(1 + pi.*W./h);
Z01 = sqrt(mu0./(ereff.*e0))./Fg;

%Conductance of Rectangular Aperture
GL = (W./(120.*lambda0)).*(1 -
(1/24).*(2.*pi.*f.*sqrt(mu0.*e0).*h).^2);

%Feedpoint Impedance of Patch Antenna
Zaa = 0.25.*((1./GL) + Z01.^2.*GL);

plot(W.*100,Zaa)
xlabel('Width (cm)')
ylabel('Feedpoint Impedance (Ohms)')
Title('Feedpoint Impedance vs. Width for 1.5GHz Rectangular Patch An-
tenna')
```

Square Patch Dimensions.m

```
clear all; close all;

%Design Constants
v = sqrt(4*pi*10^-7*8.854*10^-12);

f = 1.5*10^9; %Center frequency of patch antenna
h = 0.00159; %Thickness of substrate
eps_r = 4.24; %Relative dielectric constant of substrate
```

```

%Vary Width from 4cm to 4.8cm
W = 0.040:0.00001:0.05;

%Effective Dielectric Constant
eps_reff = ((eps_r + 1)./2) + ((eps_r - 1)./2).*((1 + (12.*(h./W))).^-0.5);

%Fringing Field Contribution to Antenna Length
delta_L = 0.412.*h.*(((eps_reff + 0.3).*((W./h) + 0.264))./((eps_reff - 0.258).*((W./h) + 0.8)));

%Antenna Length
L = (1./(2.*f.*sqrt(eps_r).*v)) - 2.*delta_L;

%Solve for L = W
x = abs((W-L).*100);

find (x < 0.00001)

plot(W.*100,L.*100,'b-')
xlabel('Width (cm)')
ylabel('Length (cm)')
title('Length vs. Width for a 1.5GHz Square Patch Antenna')

```

Square Patch Feedpoint.m

```

clear all; close all;

%Define Constants
er = 4.24;          %relative dielectric constant
mu0 = 4*pi*10^-7;
e0 = 8.854*10^-12;
f = 1.5*10^9;      %Center frequency of antenna
h = 0.00159        %thickness (m)
lambda0 = 1/(sqrt(mu0*e0*er)*f); %Wavelength (m)

theta = 0.1:0.01:pi;

%Width of Antenna (m)
W = 0.0471;

%Relative Dielectric Constant (from Empirically-Determined Formula [1])
ereff = (er + 1)/2 + ((er - 1)/2).*(1 + 12.*(h./W)).^-0.5;

%Characteristic Impedance of Transmission Line
Fg = 2.*W./h + 2/pi + (2./pi).*log(1 + pi.*W./h);
Z01 = sqrt(mu0./(ereff.*e0))./Fg;

Y01 = 1./Z01;

%Conductance of Rectangular Aperture

```

```

GL = (W./(120.*lambda0)).*(1 -
(1/24).*(2.*pi.*f.*sqrt(mu0.*e0).*h).^2);

%Feedpoint Admittance/Impedance of Patch Antenna
Yaa = Y01.*((GL + i.*Y01.*tan(theta))./(Y01 + i.*GL.*tan(theta)))...
      + Y01.*((GL + i.*Y01.*tan(pi - theta))./(Y01 + i.*GL.*tan(pi -
theta)));

Zaa = 1./Yaa;

plot((theta.*180./pi),real(Zaa))
xlabel('Theta (Degrees)')
ylabel('Resistive part of Feedpoint Impedance (Ohms)')
Title('Resistive part of Feedpoint Impedance vs. Theta')
figure(2)
plot((theta.*180./pi),imag(Zaa))
xlabel('Theta (Degrees)')
ylabel('Reactive part of Feedpoint Impedance (Ohms)')
Title('Reactive part of Feedpoint Impedance vs. Theta')
axis([0 180 -10^-10 10^-10])

```